Seismic Control of Power Transmission Tower Using Pounding TMD

Peng Zhang[1]; Gangbing Song[2]; Hong-Nan Li, M.ASCE[3]; and You-Xin Lin[4]

Abstract: Lattice transmission towers are vital components of transmission line systems, which play an important role in the operation of electrical power systems. This paper proposes a new type of tuned mass damper (TMD), the pounding tuned mass damper (PTMD), to upgrade the seismic resistant performance of a transmission tower. In the PTMD, a limiting collar with viscoelastic material laced on the inner rim is installed to restrict the stroke of the TMD and to dissipate energy through collision. The pounding force is modeled based on the Hertz contact law, whereas the pounding stiffness β is estimated in a small-scale test. A multimass model of a 55-m tower is established to verify the effectiveness of the PTMD numerically. Harmonic excitation and time-history analysis demonstrate the PTMD's superiority over the traditional TMD. Finally, a parametric study is performed for the optimal design. **DOI: 10.1061/(ASCE)EM.1943-7889.0000576.**

CE Database subject headings: Electric transmission structures; Seismic design; Energy dissipation; Earthquake engineering; Structural control; Damping; Earthquake resistant structures; Impact forces; Impact tests.

Author keywords: Seismic design; Energy dissipation; Earthquake engineering; Structural control; Damping; Earthquake-resistant structures; Impact forces; Impact tests.

Introduction

The high-voltage transmission tower, a vital component in the power transmission system, plays an important role in the development of economies and societies. Structural design of the tower is mainly governed by wind loads acting on the conductors'/towers' body, self-weight of the conductors/tower, and other loads because of icing, line deviation, broken-wire conditions, erection, and maintenance (Prasad Rao et al. 2010, 2012). However, recent investigations have reported several tower failures as a result of seismic hazard. During the Chi-Chi earthquake (1999), transmission towers and lines were severely damaged. Many transmission lines were broken, and some of the transmission towers collapsed (Yin et al. 2005). During the Wenchuan earthquake (2008), more than 20 towers collapsed and 16 towers were partially damaged (Zhang et al. 2008). Failure of electrical systems may delay emergency rescue, perhaps resulting in secondary disasters. It is of great importance to reduce the vibrational response and improve the reliability of power transmission towers under earthquakes.

To date, most retrofitting practices for transmission towers use only static approaches, such as increasing the member section area or shortening the effective member length by additional members (Park et al. 2007). However, vibration control techniques, which are already widely used in building structures, are more effective to mitigate the oscillation induced by a load of a lot of dynamic components. Many methods have been proposed to improve wind-resistant performance during the last decade.

One method is to enlarge the damping ratio by incorporating energy dissipating dampers. Park et al. (2007) proposed two types of friction-type reinforcing members and verified their performance through cyclic loading tests. Chen et al. (2008) installed magneto rheological (MR) dampers in a 108.7-m tower, a semiactive control strategy based on constant increments of a controllable damper force. Li and Yin (2008) developed a lead viscoelastic damper and verified its performance based on two practical projects. Guo et al. (2009) proposed viscoelastic dampers (VEDs) as the passive energy-absorbing devices and proposed a hybrid genetic algorithm to obtain the optimal location of the damper. These techniques aim at enhancing the energy dissipation capacity of the tower. Nevertheless, these dampers were installed only along some of the steel members because of the cost. Position optimization is a complex and time-consuming procedure. Moreover, these devices only work when there is relative motion between the two ends of the damper. The energy dissipation capacity is limited by the motion intensity of the tower.

Another method is to apply dynamic absorbers. Kilroe (2000) installed vibration absorbers on the members of tower arms to mitigate the fatigue phenomena. Battista et al. (2003) proposed a nonlinear pendulum-like damper, which reached reduction efficiency by over 90% with the first mode of vibration. Liu and Li (2008) combined the linear spring model and the Maxwell model to simulate the tuned mass damper (TMD) in a three-dimensional tower model. Numerical results showed that the vibrational response was reduced by 17% with optimal design. The superiority of an energy-absorbing device lies in its low cost and easy installation. Nevertheless, it mainly abates the tuned modes of vibration and is often helpless to suppress higher-order mode oscillations (Qu et al. 2001).

Both TMDs and VEDs were successfully combined, utilizing their respective advantages. Deng et al. (2002) used the TMD to

[1]Ph.D. Candidate, Faculty of Infrastructure Engineering, Dalian Univ. of Technology, Ganjingzi District, Dalian, Liaoning 116024, China. E-mail: peng1618@163.com

[2]Professor, Dept. of Mechanical Engineering, Univ. of Houston, Houston, TX 77004 (corresponding author). E-mail: GSong@Central.uh.edu

[3]Professor, Faculty of Infrastructure Engineering, Dalian Univ. of Technology, Ganjingzi District, Dalian, Liaoning 116024, China. E-mail: hnli@dlut.edu.cn

[4]Engineer, Guangdong Electrical Co., 8 Shuijinggang Rd., Guangzhou 510080, China. E-mail: youxinlin@163.com

Note. This manuscript was submitted on July 18, 2012; approved on December 5, 2012; published online on December 7, 2012. Discussion period open until March 1, 2014; separate discussions must be submitted for individual papers. This paper is part of the ***Journal of Engineering Mechanics***, Vol. 139, No. 10, October 1, 2013. ©ASCE, ISSN 0733-9399/2013/10-1395–1406/$25.00.

control the first mode vibration and increase the system damping by means of multiple VEDs. The study showed that the maximum value of its response was reduced by 10–20%.

To increase the effective frequency range and further reduce the amplitude of resonance, nonlinear vibration absorbers have been developed in the recent decade (Vakakis 2001; Gendelman 2001). Gendelman (2001) was the first to provide numerical simulation results of energy pumping from a directly excited linear oscillator to a nonlinear attachment. Jiang et al. (2003) studied the effect of a nonlinear energy sink (NES) on the steady-state dynamics of a weakly coupled system and found out that a NES was capable of absorbing steady-state vibration energy from a linear oscillator, localizing the energy away from the directly forced subsystem. Possible application of a NES to primary systems with multiple degrees of freedom is intensively being studied now. Gourdon and Lamarque (2005) proposed a piecewise linear system as a NES and numerically investigated its effectiveness. Gourdon et al. (2007) used two linear springs to implement cubic nonlinearity to a structure and experimentally verified the theoretical effects of energy pumping, specifically with seismic excitation.

In this paper, the pounding tuned mass damper (PTMD) is proposed as another combination of a traditional TMD and energy dissipation materials. The PTMD can also be regarded as a NES. To examine the performance of the PTMD, a pounding force model is established based on the Hertz contact law. After determining and verifying parameters by experimentation, the pounding force model is incorporated into a multidegree-freedom model of a 55-m tower for numerical study. Sinusoidal and seismic records are used to excite the incorporated model. Both the time-domain analysis and frequency domain analysis demonstrate the PTMD's superiority over a traditional TMD. In the end, effects of several parameters on the seismic-reduction performance are also investigated in a parametric study, providing a basis for the optimal PTMD design.

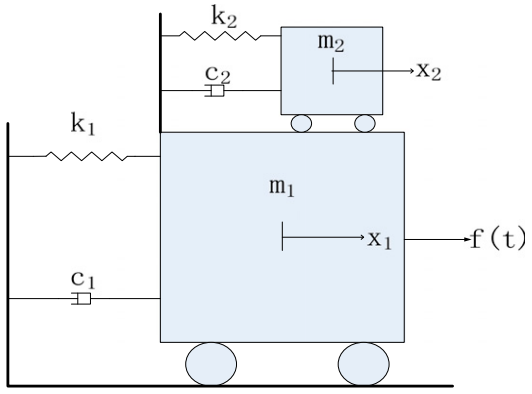

Fig. 1. Schematic model of a tuned mass damper

Schematic of a Tuned Mass Damper

The PTMD is an improvement of a traditional TMD. As illustrated in Fig. 1, a TMD is a dynamic absorber consisting of a mass, spring, and viscous damper. The TMD is often tuned so that it can vibrate at the natural frequency of the primary structure, generating an inertial force, which is the antiphase to the excitation force and attenuates the vibration of the primary structure. The motion of the TMD system is expressed in Eqs. (1) and (2)

$$m_2\ddot{x}_2 + c_2(\dot{x}_2 - \dot{x}_1) + k_2(x_2 - x_1) = 0 \tag{1}$$

$$m_1\ddot{x}_1 + c_1\dot{x}_1 + c_2(\dot{x}_1 - \dot{x}_2) + k_1x_1 + k_2(x_1 - x_2) = f \tag{2}$$

In Eq. (2), the attached TMD increases the damping and stiffness of the combined system and reduces the vibration.

Vibration mitigation performance is quite sensitive to the damping ratio of the viscous damper c_2. As shown in Fig. 2, a TMD splits the natural frequency of a primary structure into a lower and a higher frequency. If the damping is too low then resonance occurs at the two undamped resonant frequencies of the combined system (Saidi et al. 2011). If the damping is too large, the mass block may be locked and the TMD device loses the ability to absorb energy. The optimal damping ratio is given by Eqs. (3) and (4) (Rana and Soong 1998)

$$\mu = \frac{m_2}{m_1} \tag{3}$$

$$\xi_{\text{opt}} = \sqrt{\frac{3\mu}{8(1+\mu)}} \tag{4}$$

where ξ_{opt} = optimal damping ratio, and μ = mass ratio.

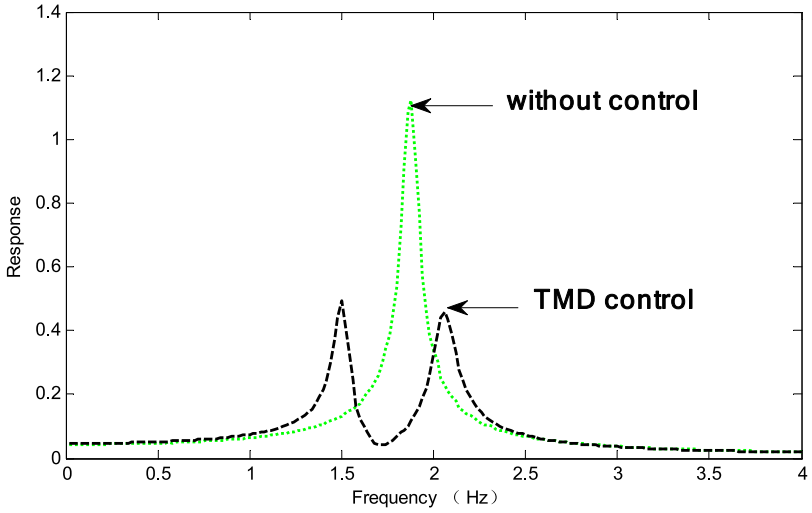

Fig. 2. Tuned mass damper control effect in the frequency domain, $\mu = 2\%$

J. Eng. Mech., 2013, 139(10): 1395-1406

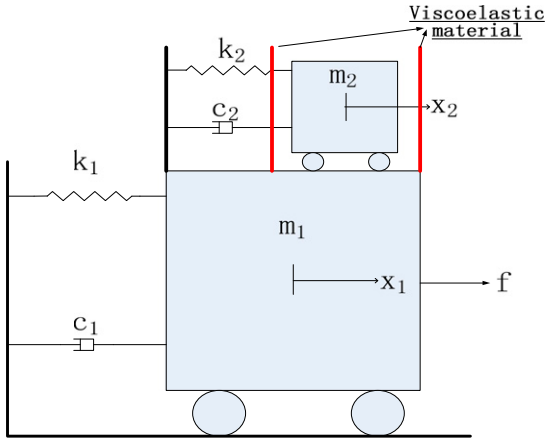

Fig. 3. Schematic model of a pounding tuned mass damper

During the last several decades, many other types of dampers have also been introduced to replace the viscous dampers, such as friction dampers (Farshi and Assadi 2011; Lin et al. 2012) and MR dampers (Weber and Maslanka 2012; Zemp et al. 2011). However, it is complicated and expensive to design, manufacture, and implement these dampers. Some dampers even demand continual maintenance (Collette 1998), which may be unrealistic because of the transmission tower's remoteness.

Another drawback of the TMD is its ineffectiveness during strong earthquakes. Because of the limitation in the installation space in real engineering structures, the TMD may get into a nonlinear phase or collide with the boundary under overintensive loads. Yan et al. (2010) extensively investigated this phenomenon and found out that the TMD is not effective if its impact parameters are not reasonably designed.

Schematic of a Pounding Tuned Mass Damper

A PTMD is a constrained TMD utilizing viscoelastic (VE) damping material. As shown in Fig. 3, the major difference between the PTMD and a traditional TMD is the additional motion limitation collar lined with VE material on the inner rim. The vibration amplitude of the structure is reduced first by transferring momentum between the structure and the added mass of the PTMD, and then the absorbed mechanical energy is dissipated as heat energy when impact occurs between the constrained mass and the VE damping material. The effectiveness of the PTMD depends on the dynamic characteristics of the TMD component, such as the stroke, the amount of added mass, and the damping properties of the damping VE material.

Fig. 4 illustrates the proposed PTMD for a transmission tower. A metal ball is hung by a cable inside a pipe. The length of the cable is determined to match the natural frequency of the tower. The pipe's inner surface is covered with VE material. When the ball impacts it, the pipe can dissipate the kinetic energy and restrict the motion of the ball.

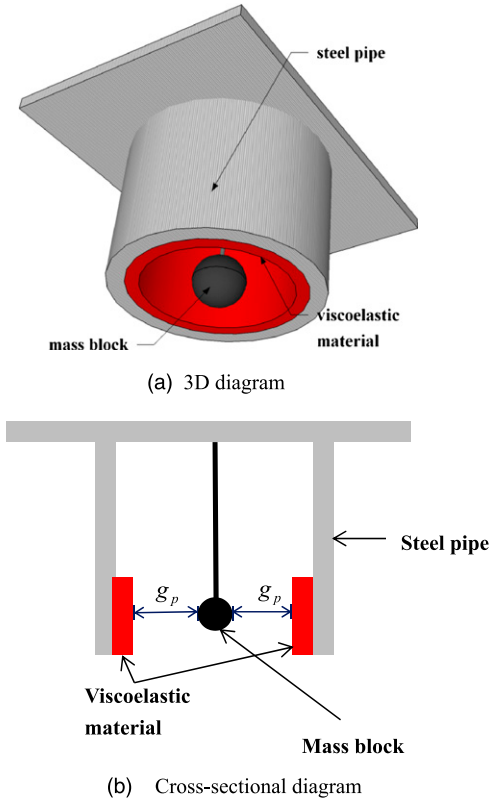

Fig. 4. Pounding tuned mass damper designed for the transmission tower: (a) three-dimensional diagram; (b) cross-section diagram

Modeling of Pounding Force

A numerical model is required to analyze the response of a structure controlled by a PTMD. During recent decades, several models have been investigated to study the impact of an adjacent building in severe earthquakes. The linear spring model (Maison and Kasai 1990, 1992; Kasai et al. 1990) was first used to represent the force during impact. However, it cannot account for energy loss during collision. The Kelvin model combined the linear spring with a damper (Wolf and Skrikerud 1980; Anagnostopoulos 1988; Jankowski et al. 1998). The damping coefficient can be determined to describe the energy dissipation. Both the linear spring model and the Kelvin model cannot describe pounding as a highly nonlinear phenomenon. Alternatively, a nonlinear spring, based on the Hertz contact law, can be used to model impact (Jing and Young 1991; Pantelides and Ma 1998; Chau and Wei 2001). The Hertz contact law is a representative of elastic impact but excludes the energy dissipation during impact. More recently, a nonlinear VE model based on the Hertz contact law, in conjunction with a damper that is active only during the approach period of impact, has been used to analyze structural pounding (Jankowski 2005). This paper adapts the Hertz contact law to simulate the pounding force

$$F = \begin{cases} \beta(x_1 - x_2 - g_p)^{3/2} + c(\dot{x}_1 - \dot{x}_2) & x_1 - x_2 - g_p > 0 \text{ and } \dot{x}_1 - \dot{x}_2 > 0 \\ \beta(x_1 - x_2 - g_p)^{3/2} & x_1 - x_2 - g_p > 0 \text{ and } \dot{x}_1 - \dot{x}_2 < 0 \\ 0 & x_1 - x_2 - g_p < 0 \end{cases} \quad (5)$$

J. Eng. Mech., 2013, 139(10): 1395-1406

where x_1 and x_2 = displacements of the pounding motion limiting collar and the mass block, respectively; g_p = gap between them; $x_1 - x_2 - g_p$ = relative pounding deformation; $\dot{x}_1 - \dot{x}_2$ = relative velocity; and β = pounding stiffness coefficient that mainly depends on material properties and the geometry of colliding bodies. Because the VE material is highly nonlinear, the impact damping c is not constant. The impact damping depends on the pounding stiffness and the deformation of the VE layer. At any instant of time its value can be obtained from Eq. (6)

$$c = 2\xi\sqrt{\beta\sqrt{x_1 - x_2 - g_p}\,\frac{m_1 m_2}{m_1 + m_2}} \tag{6}$$

$$\xi = \frac{9\sqrt{5}}{2}\frac{1 - e^2}{e[e(9\pi - 16) + 16]} \tag{7}$$

where m_1 and m_2 = masses of the two colliding bodies, and ξ = impact damping ratio correlated with the coefficient of restitution e, which is defined as the relationship between the postimpact (final) relative velocity, $\dot{x}_1^f - \dot{x}_2^f$, and the prior-impact (initial) relative velocity, $\dot{x}_1^0 - \dot{x}_2^0$, of the two colliding bodies

$$e = \frac{\left|\dot{x}_1^f - \dot{x}_2^f\right|}{\dot{x}_1^0 - \dot{x}_2^0} \tag{8}$$

The coefficient's values can be easily determined experimentally by dropping a sphere on a massive plane plate and observing the rebound height

$$e = \sqrt{h^f / h^0} \tag{9}$$

where h^0 and h^f = initial height and rebound height, respectively. The case when $e = 1$ denotes a fully elastic collision, whereas $e = 0$ stands for a perfectly plastic impact.

After assessing the value of ξ, the pounding stiffness β can be determined numerically through iterative simulations, which tend to fit the experimentally obtained pounding force time histories.

Determination of Pounding Stiffness

The only unknown parameter β of the pounding force model can be determined using the least mean square method in a small-scale experiment. Fig. 5 shows the experimental setup. The equipment consists of a TMD model, a motor with unbalanced weight, a VE pounding component, and sensors. The TMD part is made up by two steel rods of 12 mm in diameter with a copper block of 1.5 kg attached to one end. A motor is mounted on the copper block to drive the unbalanced weight. Seven layers of 3M VHB4936 tape adhere to the surface of an aluminum semiring. Beneath the semiring, a PCB 208B02 force sensor is installed to measure the axial pounding force. The signal conditioner PCB484B is connected to the force sensor. Another sensor used is the Keyence Lbl1 laser sensor, which is placed 100 mm beneath the mass block to measure the displacement of the mass. A data acquisition system (*dSPACE* 1104) is used to acquire data, and the sampling interval is 0.001 s. The test is conducted at room temperature. The attained force and displacement are plotted in Fig. 6.

A force model, as expressed in Eqs. (5–9), is established in *MATLAB/Simulink*. The pounding stiffness β is estimated using the least mean square (LMS) optimization method. The value of β is

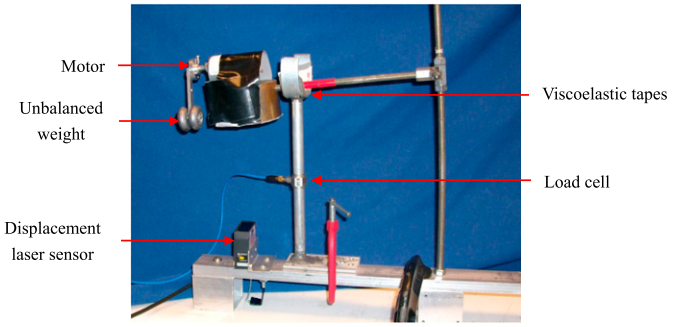

Fig. 5. Experimental setup

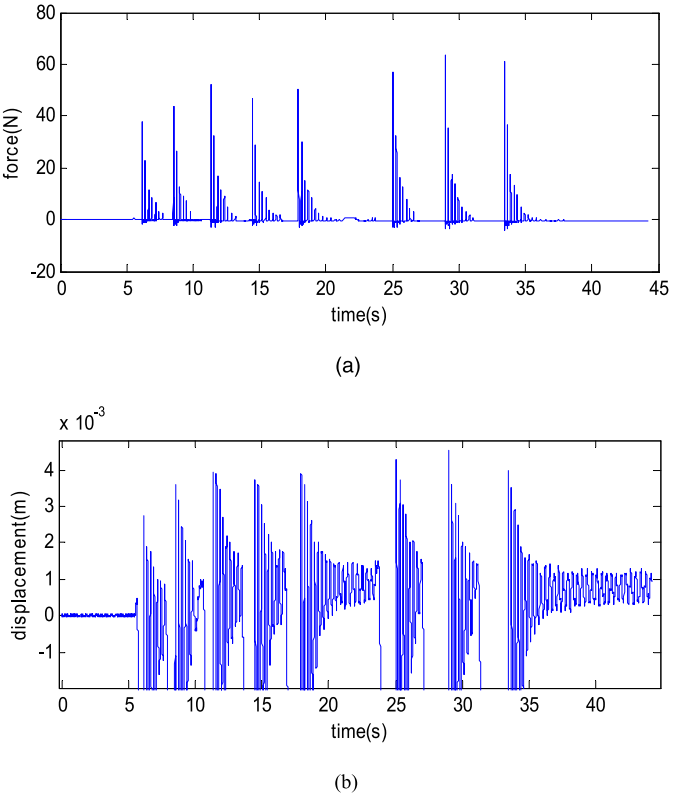

Fig. 6. Experimental result: (a) time history of force; (b) time history of displacement

1.7×10^4 N/m$^{3/2}$. It's very small compared with that of concrete to concrete impact (1.13×10^9 N/m$^{3/2}$) or steel to steel impact (4.66×10^9 N/m$^{3/2}$) (Jankowski 2005). The adhered VE material significantly reduces the pounding stiffness and increases the energy dissipation. Comparisons between the simulated pounding force and experimental value are plotted in Fig. 7.

Modeling of the Power Transmission Tower

A SZ21-type tangent transmission tower illustrated in Fig. 8(a) is chosen to verify the PTMD's effectiveness. This tower is made of Q345 angle steels connected with bolts. Its height is 53.9 m, and its weight is 19 t.

Fig. 8(b) shows the finite-element (FE) model of the transmission tower developed in the commercial FEM software, *SAP2000*. The entire FE model consists of 618 nodes and 1,588 elements, and the

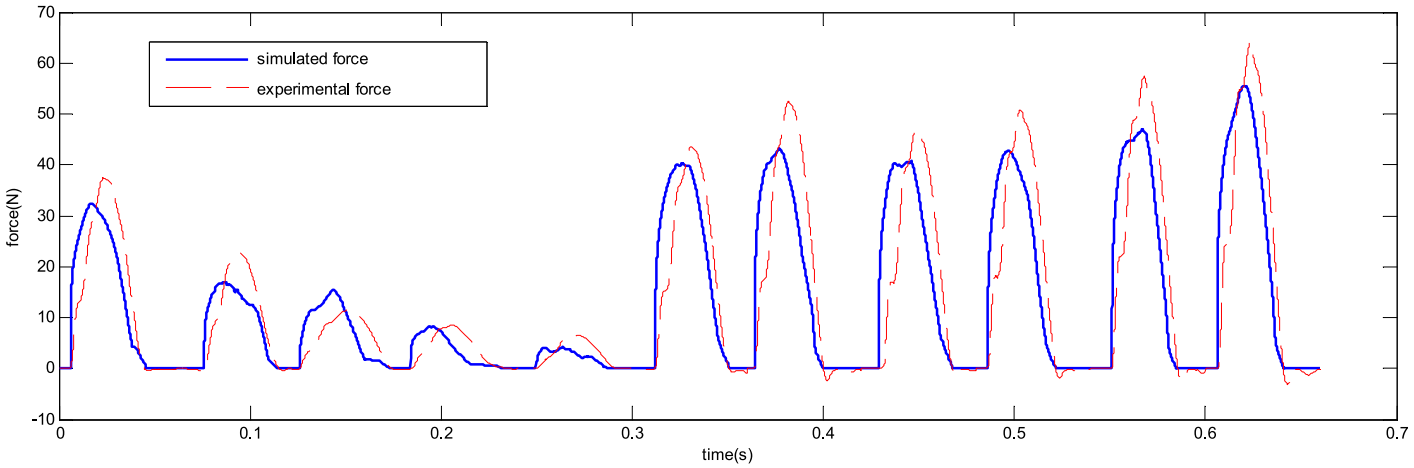

Fig. 7. Validation of pounding force

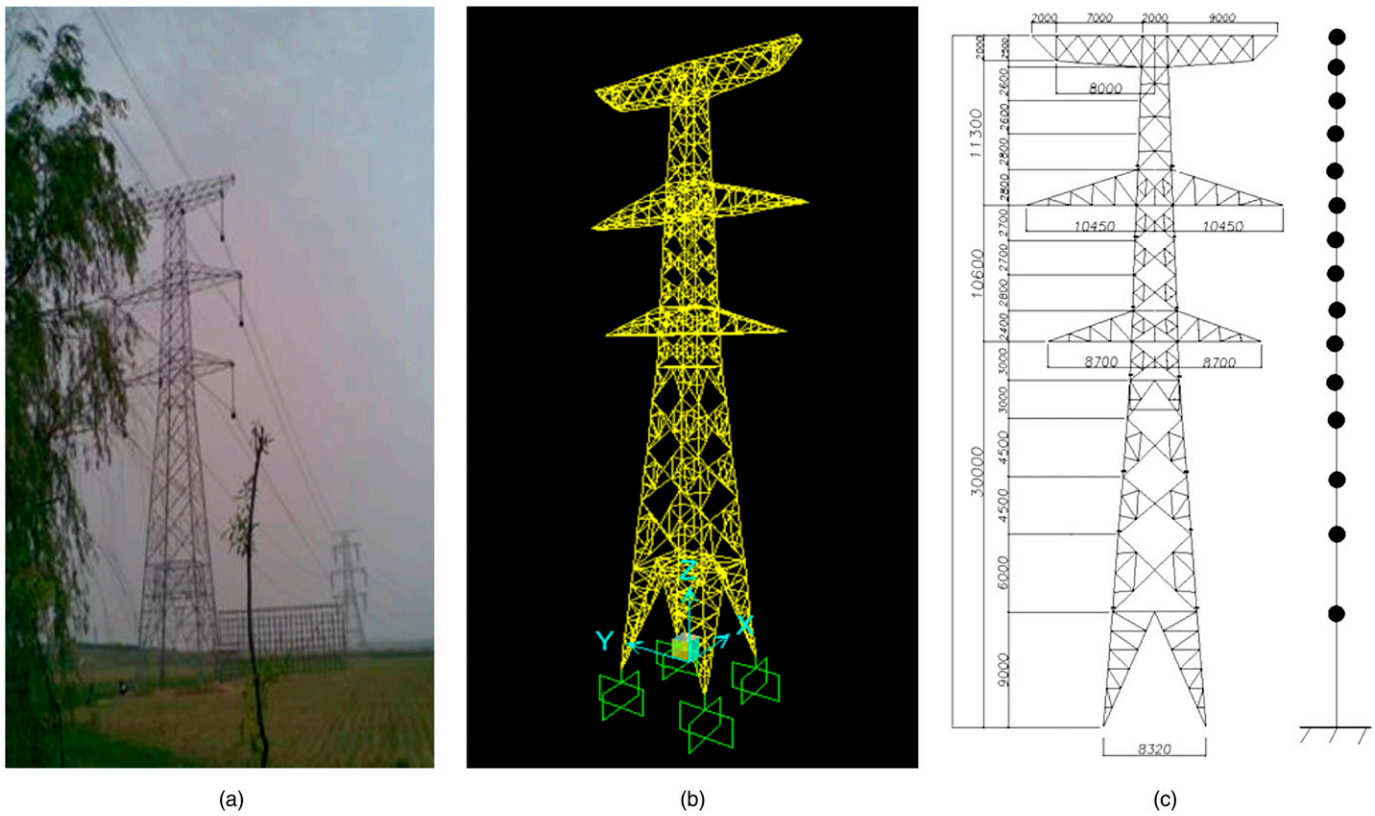

Fig. 8. A 55-m SZ21-type tangent transmission tower: (a) real tower; (b) *SAP2000* FEM model; (c) simplified model

natural frequency is 1.84 Hz. Because it is impossible to implement a nonlinear pounding force into the *SAP2000* software; a simplified multimass model is established based on the FEM model, as shown in Fig. 8(c). The stiffness matrix of the simplified model is computed as the inverse of the flexibility matrix determined based on the FEM model. Although the total degree of freedom is reduced from 3,708 to 15, the first natural frequency is almost the same: 1.87 Hz, only 1.6% higher than the FEM model. For further verification, these two models are subjected to a recorded accelerogram, the S00E component of the 1940 Imperial Valley earthquake at the El Centro Site in California. The peak ground motion is scaled to 400 cm/s^2. Fig. 9 illustrates the time history of the top displacement. The error is negligibly small.

Control Performance Study

Dynamic Equations of the System

The equation of motion of the tower-PTMD system can be expressed as

$$M\ddot{x}(t) + C\dot{x}(t) + Kx(t) = -M\Lambda x_g(t) + H\Gamma F(t) \qquad (10)$$

where $\ddot{x}(t)$, $\dot{x}(t)$, and $x(t)$ = acceleration, velocity, and displacement of the tower and PTMD, respectively; $\ddot{x}_g(t)$ = ground acceleration; $F(t)$ = pounding force calculated by Eq. (5); and M, C, and $K = (16 \times 16)$ mass, damping, and stiffness matrices, respectively

J. Eng. Mech., 2013, 139(10): 1395-1406

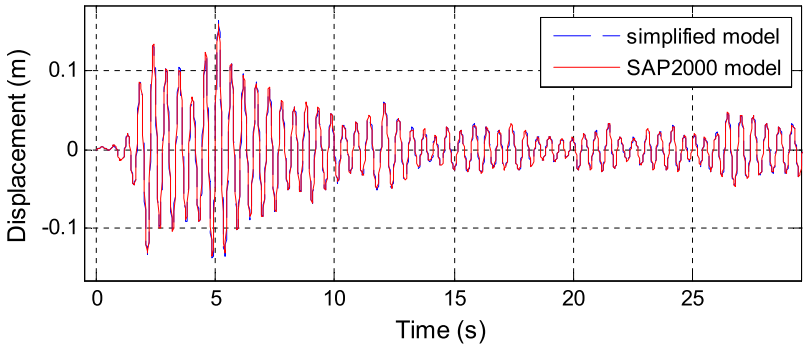

Fig. 9. Verification of the simplified model, displacement response of the tower under the El Centro earthquake

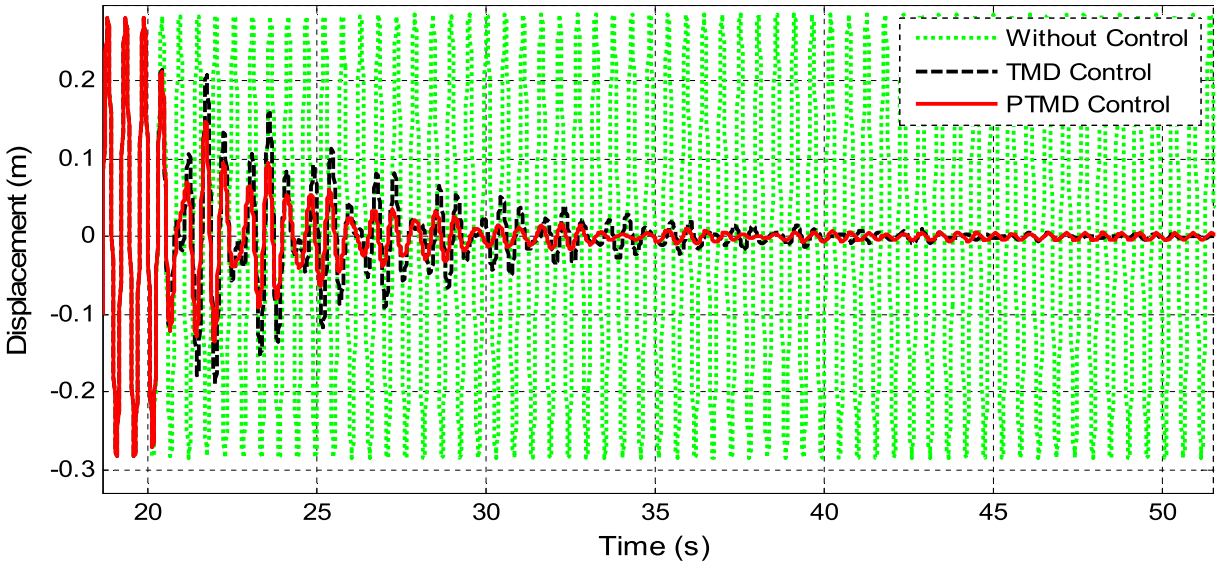

Fig. 10. Displacement response under resonance excitation

$$M = \begin{bmatrix} M_s & 0 \\ 0 & m_d \end{bmatrix}, \quad C = \begin{bmatrix} C_s & C_c \\ sym & c_d \end{bmatrix}, \quad K = \begin{bmatrix} K_s & K_c \\ sym & k_d \end{bmatrix} \tag{11}$$

where M_s, C_s, and K_s = previously calculated mass, damping, and stiffness matrices of the tower structure, respectively; m_d, c_d, and k_d = mass, damping, and stiffness of the damper, respectively; and C_c and K_c = coupling matrices of the damping matrix and stiffness matrix, respectively. The PTMD is added to Node 15; therefore, C_c and K_c are defined as

$$C_{c\ (15\times1)} = [0, \ldots, 0, -C_d]^t \tag{12}$$

$$K_{c\ (15\times1)} = [0, \ldots, 0, -K_d]^t \tag{13}$$

In Eq. (10), Λ is a column vector of ones, Γ denotes the location of the pounding force, and H is defined to determine the direction of the pounding force

$$H = \begin{cases} 1 & x_d - x_{15} - g_p > 0 \\ -1 & x_d - x_{15} - g_p < 0 \\ 0 & \text{otherwise} \end{cases} \tag{14}$$

where x_d and x_{15} = displacements of the damper and top node of the tower, respectively; and g_p = gap between the mass block and the VE material.

Effectiveness of the Pounding Tuned Mass Damper under Harmonic Ground Motion

The performance of the PTMD is first evaluated under the sinusoidal excitation. In Fig. 10, the tower is subjected to the resonance frequency (1.87 Hz) for 20 s. Afterward, the traditional TMD and PTMD are applied. The two techniques can both reduce the harmonic responses by more than 90%. However, the PTMD can incorporate greater damping effectiveness. After 10 s, the displacement with the PTMD control is reduced to 2.3 cm, almost the steady-state response. Nevertheless, it takes 20 s for the TMD to achieve the same result.

Fig. 11 shows the vibration control effect in the frequency domain. Both the two control devices split the natural frequency into a lower and upper natural frequency. The control devices reduce the response amplitude at the resonance frequency but may also increase the response amplitude at other frequencies. The amplitude response of the PTMD is smaller than the TMD at every frequency.

Effectiveness of the Tuned Mass Damper under Recorded Accelerogram

The previously described tower was subjected to two earthquakes: El Centro and Kobe earthquakes. For consistent comparisons, the two records are scaled to the peak acceleration of 400 cm/s^2. The mass ratio of both the TMD and PTMD is taken as 2%. The

J. Eng. Mech., 2013, 139(10): 1395-1406

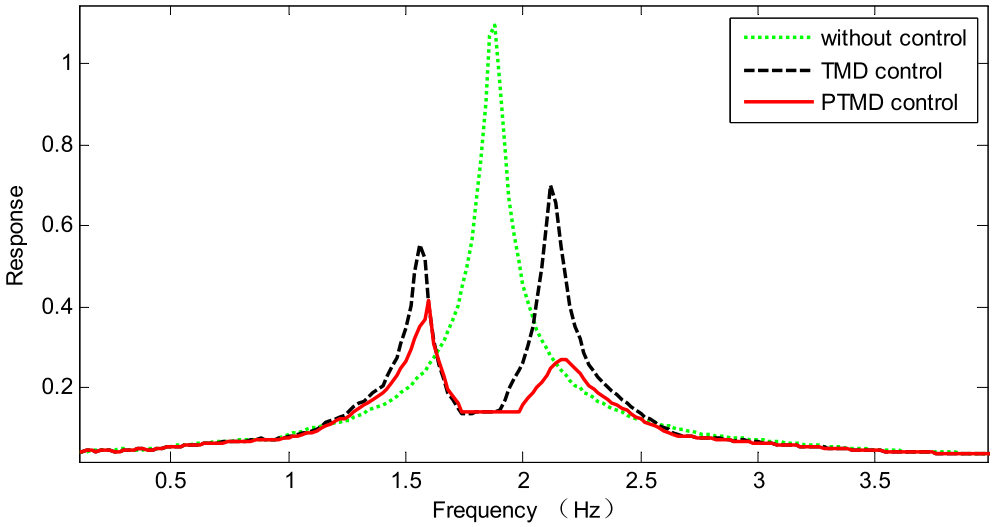

Fig. 11. Displacement response in the frequency domain

damping ratio is 2%. The gap between the mass block and VE material is 0.05 m.

Reduction ratios are defined to evaluate the performance of the traditional TMD and the PTMD

$$\eta_d = \frac{D_0 - D_{\text{ctrl}}}{D_0} \times 100\% \tag{15}$$

$$\eta_a = \frac{\text{Acc}_0 - \text{Acc}_{\text{ctrl}}}{\text{Acc}_0} \times 100\% \tag{16}$$

$$\eta_f = \frac{F_0 - F_{\text{ctrl}}}{F_0} \times 100\% \tag{17}$$

where D_{ctrl} and D_0 = displacement responses of the tower with and without control devices, respectively; Acc_{ctrl} and Acc_0 = acceleration at the top of the tower with and without control devices, respectively; and F_{ctrl} and F_0 = axial internal force of the tower with and without control devices, respectively. They can be the maximum value or the RMS value.

Analysis of the top displacement of the tower under the El Centro earthquake is shown in Fig. 12(a). Although the regular TMD significantly reduced the peak value by 21.0%, a larger reduction ratio of 41.2% is achieved by the PTMD. From 6 to 12 s, the displacement with the control device is larger than that without the control device. This can be explained by the principle of the TMD in terms of energy. The TMD is designed to absorb kinetic energy from the primary structure. When the oscillation of the tower diminishes gradually, the energy is transmitted back, aggregating the vibration. The PTMD is more effective than the regular TMD, because it introduces the massive energy dissipation during impact. In Fig. 12(a), the displacement of the PTMD is always smaller than the regular TMD, and the RMS reduction ratio is 57.5%, greater than that of the TMD, which is 13.4%.

In terms of top acceleration, as shown in Fig. 12(b), greater effective mitigation is achieved by the PTMD having a maximum value reduced by 34.3% and a RMS reduction of 45.2%. Generally, the control effect of the displacement is larger than the acceleration.

In terms of axial internal force, greater effective performance has also been observed with the PTMD. In Fig. 12(c), the largest axial internal force at the tower bottom is reduced by 43.7% during the El Centro earthquake. This is followed by the TMD's reduction of 37.1%. For members above 40 m, the axial internal forces are no more than half of the members near the bottom. They are not effectively reduced by either device.

The results similar to Fig. 12 are also observed in Fig. 13, which denotes the response under the 1995 Kobe earthquake. The maximum displacement, acceleration, and axial internal force are reduced by 30.0, 20.2, and 35.6%, respectively, with the application of the PTMD, whereas the reduction ratios of the TMD are only 10.9, 0.4, and 26.3%, respectively. These results can be found in Table 1.

Parametric Study

To obtain a rational design of the PTMD, the effects of its pounding stiffness, β, the gap between the mass block and VE material, g_p, the mass ratio of the TMD over the tower, μ, and the intensity of the earthquake are discussed. Unless mentioned otherwise, the following nominal values are assumed for the present numerical study: $\beta = 17{,}259\ \text{N/m}^{3/2}$, $g_p = 0.05$ m, $\mu = 2\%$, and the intensity is still 400 cm/s^2.

Pounding Stiffness

The pounding stiffness, the key parameter in modeling the pounding force, is determined by material properties and the geometry of colliding bodies. It ranges from 15,000 to 30,000 $\text{N/m}^{3/2}$ during the fatigue test. Depicted in Fig. 14 are the variations of the top displacement with different pounding stiffness under the El Centro earthquake. The displacement decreases with decreasing stiffness. However, the improvement of response reduction is no more than 10%. Therefore, the PTMD control performance is not sensitive to the variation of pounding stiffness.

Gap

In terms of energy, the PTMD is adopted to absorb the kinetic energy from the tower and dissipate this energy during impact. The gap between the mass block and the VE material will influence the PTMD's performance both in absorbing and dissipating. For the larger ground acceleration, the TMD and the tower oscillate more

J. Eng. Mech., 2013, 139(10): 1395-1406

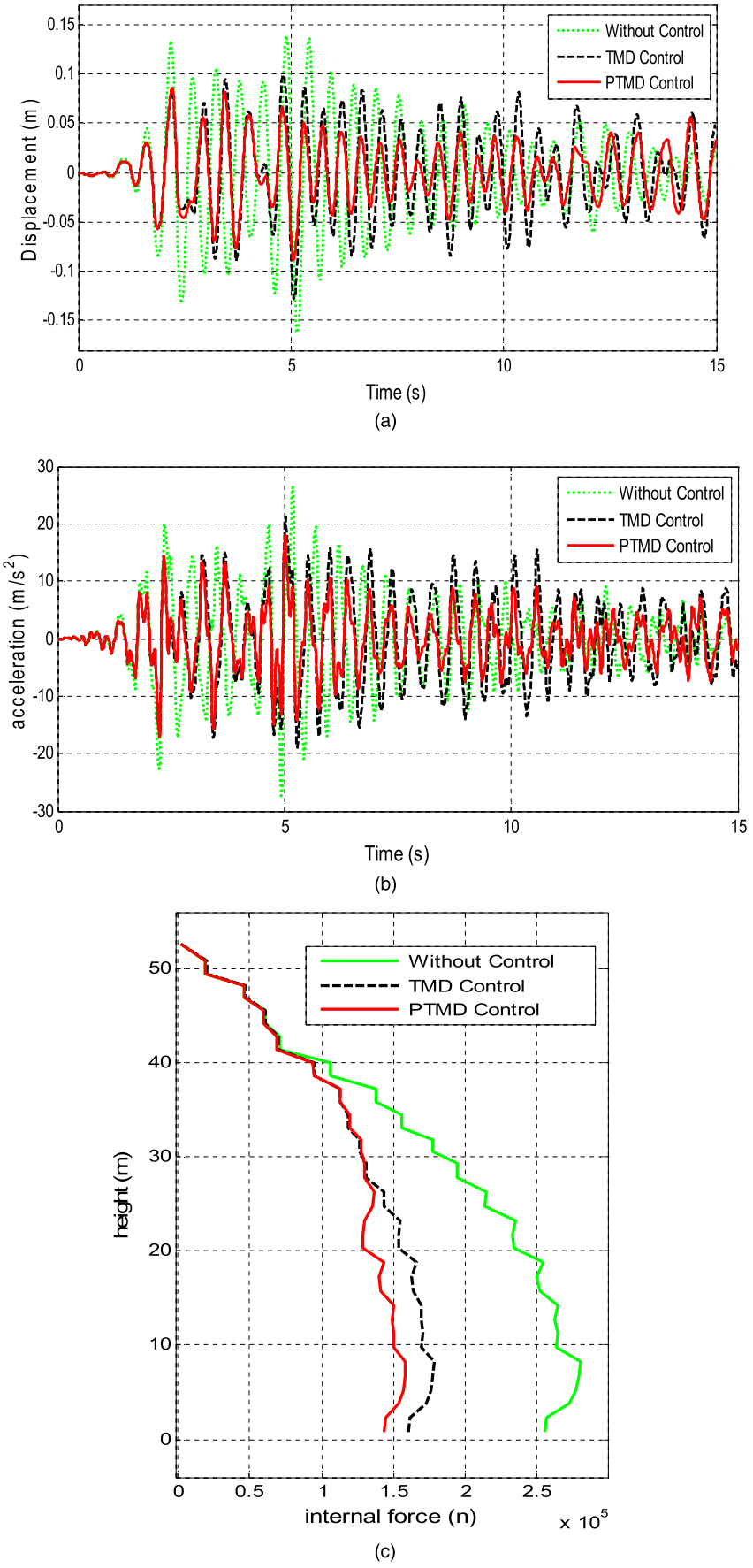

Fig. 12. Dynamic response under the El Centro earthquake: (a) displacement; (b) acceleration; (c) axial internal force

J. Eng. Mech., 2013, 139(10): 1395-1406

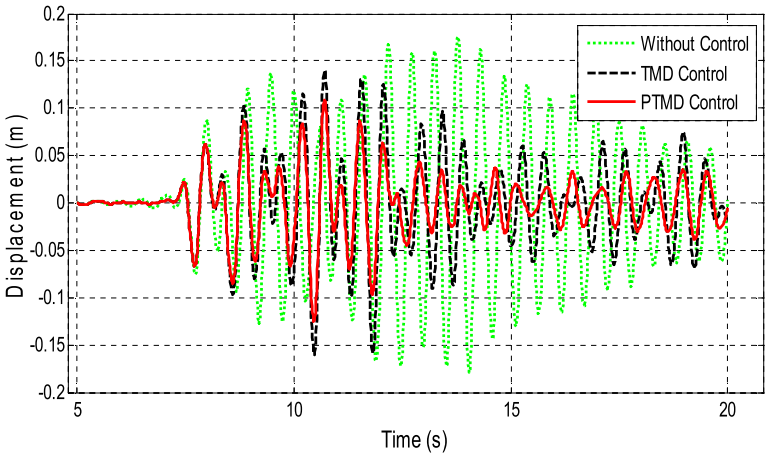

(a)

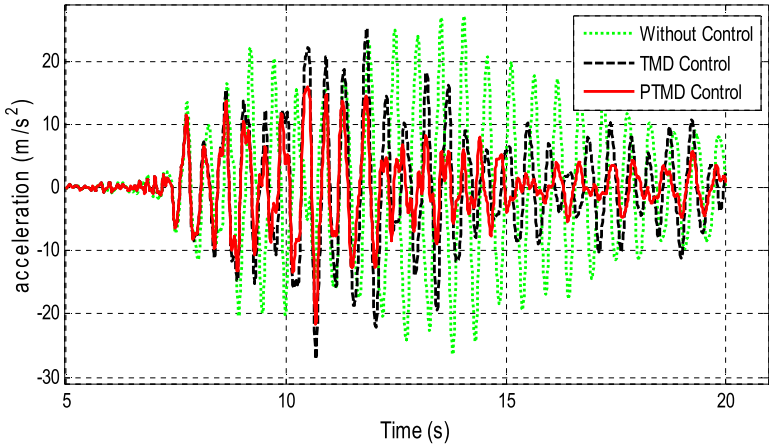

(b)

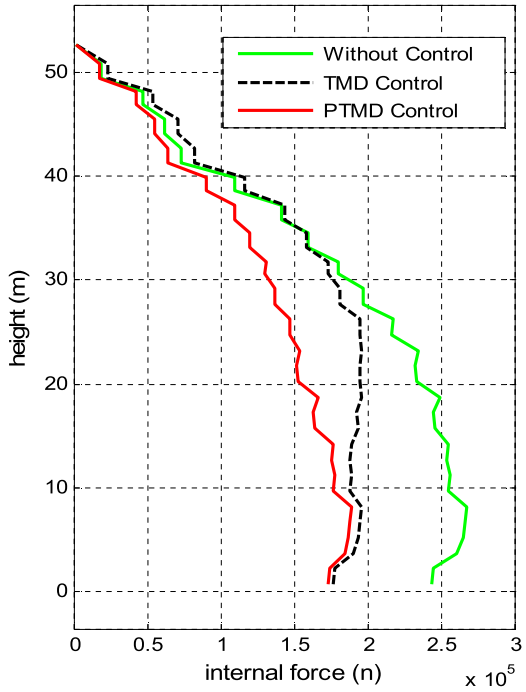

(c)

Fig. 13. Dynamic response under the Kobe earthquake: (a) displacement; (b) acceleration; (c) axial internal force

J. Eng. Mech., 2013, 139(10): 1395-1406

severely and a large gap is needed for the mass block to get into the large motion. However, the collision may not take place under the low motion with the exceedingly large gap. Thus, there is an optimal gap for every case. The optimal gap is determined by the mass ratio and intensity of the earthquake.

The variations of response reduction of the PTMD with the different gap and mass ratios under the El Centro earthquake are plotted in Fig. 15. With increasing mass ratio, the mass block vibrates less severely and the optimal gap is reduced. When the mass ratio is 1%, the optimal gap is more than 10 cm, whereas when the optimal gap is 2.2 cm, the mass ratio is 3%. Moreover, the gap can be selected within a wide range. One example is the case of the 2% mass ratio. At optimal gap, the control performance is 41.2%. Peak displacement can also be reduced by 40% if the gap is reduced by 3.5 cm from the optimal value.

In Fig. 16, the control performance is drawn based on different seismic intensities. The larger gap is needed under more severe ground motion. When the intensity of the El Centro earthquake

Table 1. Vibration Reduction Ratio

		η_d		η_a		η_f	
Earthquake		Peak (%)	RMS (%)	Peak (%)	RMS (%)	Peak (%)	RMS (%)
El Centro	Pounding tuned mass damper	41.2	57.5	34.3	45.2	43.7	48.9
	Tuned mass damper	21.0	13.4	22.2	—	37.1	24.5
Kobe	Pounding tuned mass damper	30.0	80.0	20.2	76.8	35.6	73.9
	Tuned mass damper	10.9	51.5	0.4	35.2	26.3	49.5

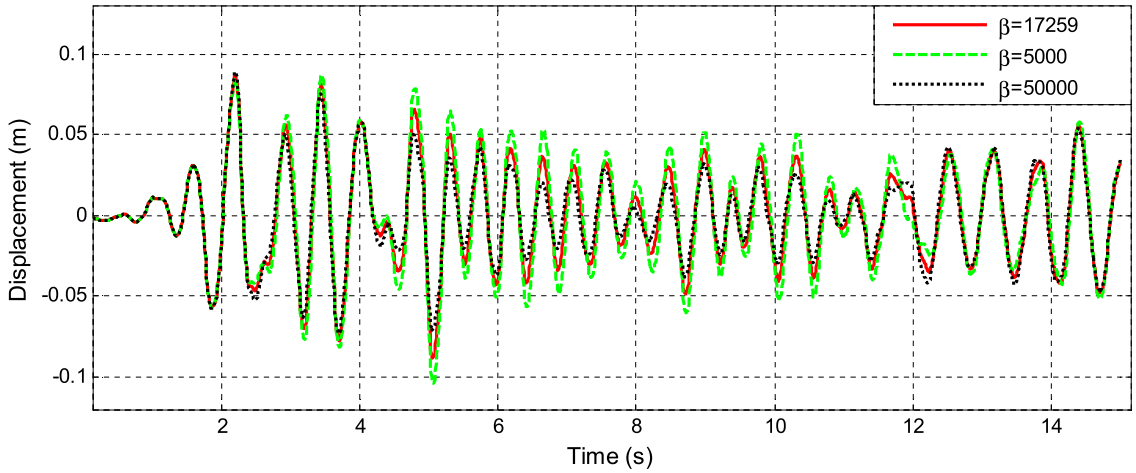

Fig. 14. Control performance comparison of different pounding stiffness under the El Centro earthquake

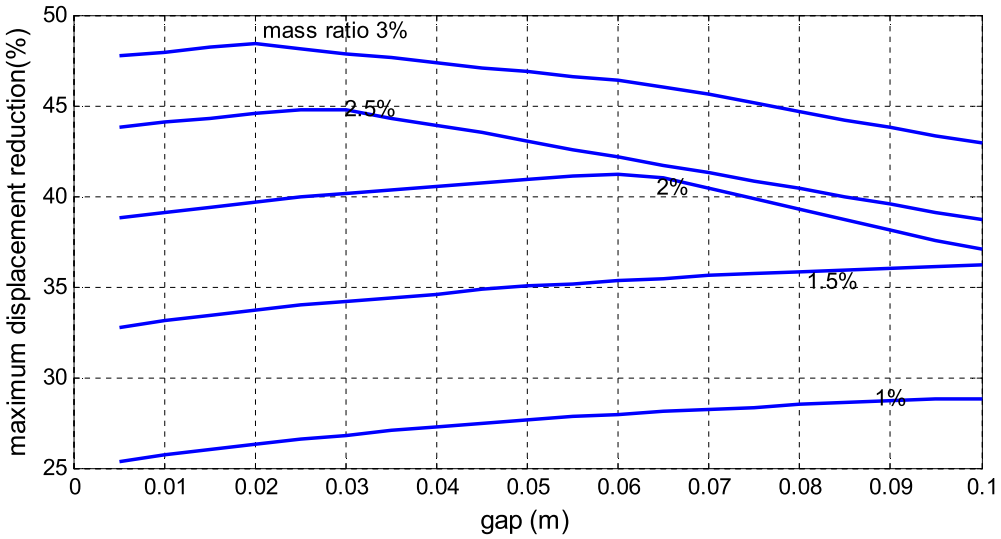

Fig. 15. Optimal gap with different mass ratio

J. Eng. Mech., 2013, 139(10): 1395-1406

increases from 100 to 800 cm/s^2, the optimal gap also increases from 2 to 16 cm.

Mass Ratio

Increasing the mass ratio can improve the reduction performance, but there is an economic mass ratio, beyond which adding more mass can only slightly improve performance. As illustrated in Fig. 15, the vibration reduction ratio increases significantly to 41.2%, whereas the mass ratio increases to 2%. Afterward, the performance improves by less than 10% by adding 1% more mass. In the TMD design, 1–2% (Saidi et al. 2011) is recommended as the mass ratio. This value can also be used for the PTMD.

Intensity

Fig. 16 illustrates the effect of seismic intensity on control performance. The PTMD reduces oscillation comparatively under more severe ground motion. This is different from the TMD, which has the limited vibration mitigation ability under a heavier motion (Yan et al. 2010).

Damping Ratio of the Tower

As given in Table 2, the PTMD reduces the oscillation more effectively if the structure has a lower damping ratio. Compared with the TMD, the PTMD can suppress the maximum displacement by 25.9% more than the TMD with 0.5% damping, whereas when the damping ratio of the tower is 5%, the PTMD is only 8.9% more effective. The TMD has very limited energy dissipation. Structures with higher damping can compensate for this disadvantage, but for structures with low damping, the PTMD is a better control method.

Concluding Remarks

In this paper, an innovative TMD, the pounding TMD, is proposed for the suppression of seismic-induced vibration of a transmission tower. The VE material is adopted to dissipate the energy absorbed by the TMD through collision. The pounding force model is established based on the Hertz contact law. The pounding stiffness is estimated using the LMS optimization method experimentally.

This paper establishes a simplified model of a 55-m SZ21-type tangent transmission tower to study the performance of the PTMD. The modal analysis and seismic response verify the accuracy of this simplified model. Numerical results indicate that the PTMD is more effective than the traditional TMD. The maximum and RMS values of the displacement, acceleration, and axial internal force are all reduced more effectively by the PTMD than the traditional TMD.

Parameter studies discuss the effects of pounding stiffness, gap, mass, intensity, and damping ratio of the tower on the reduction performance. The pounding stiffness has little influence on the control performance. With the maximum optimal mass ratio at 2%, the PTMD is more effective at reducing dynamic excitation then the traditional TMD. A mass ratio higher than 2% results in diminishing returns, where increasing the mass ratio becomes uneconomical.

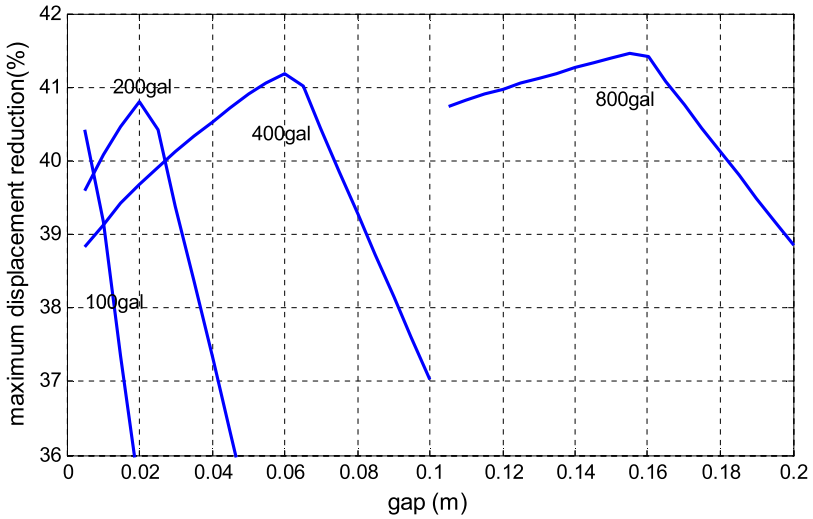

Fig. 16. Optimal gap under an earthquake with different intensity

Table 2. Vibration Reduction Comparison with Different Damping Ratio

Damping ratio (%)	Maximum response	Without control	Tuned mass damper control		Pounding tuned mass damper control	
			Response	η_d or η_a (%)	Response	η_d or η_a (%)
0.5	Displacement (m)	0.217	0.158	27.3	0.101	53.2
	Acceleration (m/s^2)	34.45	26.64	22.7	20.13	41.6
2	Displacement (m)	0.163	0.129	21.0	0.095	41.6
	Acceleration (m/s^2)	27.39	21.32	22.2	17.74	35.2
5	Displacement (m)	0.1160	0.0898	22.6	0.0795	31.5
	Acceleration (m/s^2)	19.63	14.37	26.8	14.78	24.7

J. Eng. Mech., 2013, 139(10): 1395-1406

The PTMD also can achieve better performance for structures of a lower damping ratio or under an earthquake of higher intensity.

Acknowledgments

This research work was supported by the Science Fund for Creative Research Groups of the National Natural Science Foundation of China (Grant No. 51121005) and the National Natural Science Foundation of China (Grant No. 51108059).

References

Anagnostopoulos, S. A. (1988). "Pounding of buildings in series during earthquakes." *Earthq. Eng. Struct. Dynam.*, 16(3), 443–456.

Battista, R. C., Rodrigues, R. S., and Pfeil, M. S. (2003). "Dynamics behavior and stability of transmission line tower under wind forces." *J. Wind Eng. Ind. Aerodyn.*, 91(8), 1051–1067.

Chau, K. T., and Wei, X. X. (2001). "Pounding of structures modelled as non-linear impacts of two oscillators." *Earthq. Eng. Struct. Dynam.*, 30(5), 633–651.

Chen, B., Zheng, J., and Qu, W. L. (2008). "Wind-induced response mitigation of transmission tower-line system by using magneto rheological dampers." *J. Vibrat. Shock*, 27(3), 71–74.

Collette, F. S. (1998). "A combined tuned absorber and pendulum impact damper under random excitation." *J. Sound Vib.*, 216(2), 199–213.

Deng, H. Z., Zhu, S. Y., and Wang, Z. M. (2002). "Control on wind vibration for transmission tower-line system of large crossing." *Electric Power Constr.*, 23(8), 30–37.

Farshi, B., and Assadi, A. (2011). "Development of a chaotic nonlinear tuned mass damper for optimal vibration response." *Commun. Nonlinear Sci. Numer. Simul.*, 16(11), 4514–4523.

Gendelman, O. V. (2001). "Transition of energy to a nonlinear localized mode in a highly asymmetric system of two oscillators." *Nonlinear Dyn.*, 25(1–3), 237–253.

Gourdon, E., Alexander, N. A., Taylor, C. A., Lamarque, C. H., and Pernot, S. (2007). "Nonlinear energy pumping under transient forcing with strongly nonlinear coupling: Theoretical and experimental results." *J. Sound Vibrat.*, 300(3–5), 522–551.

Gourdon, E., and Lamarque, C. H. (2005). "Energy pumping with various nonlinear structures: Numerical evidences." *Nonlinear Dyn.*, 40(3), 281–307.

Guo, Y., Sun, B. N., Ye, Y., Lou, W. J., and Shen, G. H. (2009). "Frequency-domain analysis on wind-induced dynamic response and vibration control of long span transmission line system." *Acta Aerodyn. Sinica*, 27(3), 288–295.

Jankowski, R. (2005). "Non-linear viscoelastic modeling of earthquake-induced structural pounding." *Earthq. Eng. Struct. Dynam.*, 34(6), 595–611.

Jankowski, R., Wilde, K., and Fuzino, Y. (1998). "Pounding of superstructure segments in isolated elevated bridge during earthquakes." *Earthq. Eng. Struct. Dynam.*, 27(5), 487–502.

Jiang, X., McFarland, D. M., Bergman, L. A., and Vakakis, A. F. (2003). "Steady state passive nonlinear energy pumping in coupled oscillators: Theoretical and experimental results." *Nonlinear Dyn.*, 33(1), 87–102.

Jing, H. S., and Young, M. (1991). "Impact interactions between two vibration systems under random excitation." *Earthq. Eng. Struct. Dynam.*, 20(7), 667–681.

Kasai, K., Maison, B. F., and Patel, D. J. (1990). "An earthquake analysis for buildings subjected to a type of pounding." *Proc., 4th U.S. National Conf. Earthq. Eng.*, Vol. 2, Earthquake Engineering Research Institute, Palm Springs, CA, 289–298.

Kilroe, N. (2000). "Aerial method to mitigate vibration on transmission towers." *2000 IEEE ESMO–2000 IEEE 9th Int. Conf. on Transmission and Distribution Construction, Operation and Live-Line Maintenance Proc.*, IEEE, New York, 187–194.

Li, L., and Yin, P. (2008). "The research on wind-induced vibration control for big-span electrical transmission tower-line system." *Eng. Mech.*, (supplementary issue 2), 213–229.

Lin, G., Lin, C., Lu, L., and Ho, Y. (2012). "Experimental verification of seismic vibration control using a semi-active friction tuned mass damper." *Earthq. Eng. Struct. Dynam.*, 41(4), 813–830.

Liu, G. H., and Li, H. N. (2008). "Analysis and optimization control of wind-induced dynamic response for high-voltage transmission tower-line system." *Proc., CSEE*, 28(19), 131–137.

Maison, B. F., and Kasai, K. (1990). "Analysis for type of structural pounding." *J. Struct. Div.*, 116(4), 957–977.

Maison, B. F., and Kasai, K. (1992). "Dynamics of pounding when two buildings collide." *Earthq. Eng. Struct. Dynam.*, 21(9), 771–786.

MATLAB [Computer software]. Natick, MA, The MathWorks, Inc.

Pantelides, C. P., and Ma, X. (1998). "Linear and nonlinear pounding of structural systems." *Comp. Struct.*, 66(1), 79–92.

Park, J. H., Moon, B. W., Min, K. W., Lee, S. K., and Kim, C. K. (2007). "Cyclic loading test of friction-type reinforcing members upgrading wind-resistant performance of transmission towers." *Eng. Struct.*, 29(11), 3185–3196.

Prasad Rao, N., Samuel Knight, G. M., Lakshmanan, N., and Iyer, N. R. (2010). "Investigation of transmission line tower failures." *Eng. Fail. Anal.*, 17(5), 1127–1141.

Prasad Rao, N., Samuel Knight, G. M., Mohan, S. J., and Lakshmanan, N. (2012). "Studies on failure of transmission line towers in testing." *Eng. Struct.*, 35, 55–70.

Qu, W. L., Chen, Z. H., and Xu, Z. H. (2001). "Dynamic analysis of wind excited truss tower with friction dampers." *Comp. Struct.*, 79(32), 2817–2831.

Rana, R., and Soong, T. T. (1998). "Parametric study and simplified design of tuned mass dampers." *Eng. Struct.*, 20(3), 193–204.

Saidi, I., Gad, E. F., Wilson, J. L., and Haritos, N. (2011). "Development of passive viscoelastic damper to attenuate excessive floor vibrations." *Eng. Struct.*, 33(12), 3317–3328.

SAP2000 [Computer software]. Berkeley, CA, Computers and Structures, Inc.

Vakakis, A. F. (2001). "Inducing passive nonlinear energy sinks in vibrating systems." *J. Vibrat. Acoustics*, 123(3), 324–332.

Weber, F., and Maslanka, M. (2012). "Frequency and damping adaptation of a TMD with controlled MR damper." *Smart Mater. Struct.*, 21(5), 055011.

Wolf, J. P., and Skrikerud, P. E. (1980). "Mutual pounding of adjacent structures during earthquakes." *Nucl. Eng. Des.*, 57(2), 253–275.

Yan, A. Z., Chen, Y. J., and Teng, J. (2010). "Optimization of impact parameter of TMD based on hertz model." *Eng. Mech.*, 27, 189–193.

Yin, R. H., Li, D. L., Liu, G. L., and Zhai, T. (2005). "Seismic damage and analysis of power transmissions towers." *World Inform. Earthq. Eng.*, 21(1), 51–54.

Zemp, R., De La Llera, J. C., and Almazan, J. L. (2011). "Tall building vibration control using a TM-MR damper assembly." *Earthq. Eng. Struct. Dynam.*, 40(3), 339–354.

Zhang, Z. Y., Zhao, B., Cao, W. W., Li, Y., and Ge, Z. X. (2008). "Investigation and preliminary analysis of damages on the power grid in the Wenchuan Earthquake of M8.0." *Electric Power Technologic Economics*, 20(4).